Mathematical model and numerical simulation of conductometric biosensor of urea

Fares Zouaoui, Nadia Zine, Abdelhamid Errachid, Nicole Jaffrezic-Renault

Mathematical model and numerical simulation of conductometric biosensor of urea

*Fares ZOUAOUI, Nadia ZINE, Abdelhamid ERRACHID, Nicole JAFFREZIC-RENAULT**

*Corresponding Author**

Affiliation : University of Lyon, Institute of Analytical Sciences, UMR 5280, CNRS, 69100 Villeurbanne, France.

* e-mail: corresponding author: nicole.jaffrezic@univ-lyon1.fr

Received: ((will be filled in by the editorial sttaff))
Accepted: ((will be filled in by the editorial sttaff))

Abstract
In this article, a mathematical model was developed to describe and optimize the configuration of the urea biosensor. The biosensor is based on interdigitated gold microelectrodes modified with a urease enzyme membrane. The model presented here focuses on the enzymatic reaction and/or diffusion phenomena that occur in the enzyme membrane and in the diffusion layer. Numerical resolution of differential equations was performed using the finite difference technique. The mathematical model was validated using experimental biosensor data. The responses of the biosensor to various conditions were simulated to guide experiments, improve analytical performance, and reduce development costs.

Keywords: Conductometry; urea; urease; modelling; analytical performance.

DOI: 10.1002/elan.((will be filled in by the editorial sttaff))

1. Introduction

Urea is the breakdown product of nucleic acids and proteins into nitrogenous waste in the liver. It is eliminated from the body primarily through urine, but it is also secreted in bodily fluids such as blood and saliva [1]. Humans have a normal urea level of 0,25 to 0,6 mM in the blood and 155 to 390 mM in the urine thus providing key information on kidney function and in the diagnosis of various kidney disorders and hepatic [2]. Regarding the environment, urea is used in agriculture as a fertilizer, de-icing agent, etc. However, these molecules lead to the acidification and eutrophication of fertile soil. Thus the contamination of surface water by runoff disrupts the ecosystem and causes the death of aquatic life [3]. Therefore, it becomes necessary to monitor urea levels in urine and blood and in different fields such as agriculture, food, pharmacy, etc.

The use of enzymatic hydrolysis of urea by urease in the development of a urea biosensor has attracted considerable attention from biochemical and clinical analyzes [4]. Hydrolysis of urease in urea generates ionic products, such as NH_4^+, HCO_3^- and OH^-. The ions produced are monitored by several techniques, such as an optical transducer [5,6], potentiometry [7,8], colorimetry [9,10], amperometry [11,12], and conductometry [13,14].

Conductometric biosensors have significant advantages, as they do not require the use of a reference electrode; they operate at an alternating voltage of low amplitude, they are insensitive to light; and they can be miniaturized and integrated easily [15]. The conductometric measurement method can be used in enzymatic catalysis involves either the consumption or the production of charged species, therefore, lead to an overall change in the ionic composition of the sample tested. The conductivity measured by the biosensor is easily modified by the presence of other ions or those produced by the enzymatic reaction, which affects the selectivity of the method. However, in the case of an integrated microbiosensor, this limitation can be overcome by using a differential measurement scheme which compensates for changes in the conductivity of the medium [16].

This article aims to investigate the problem of optimizing biosensor design using an interdisciplinary approach that combines mathematical and computational modeling with electrochemical and biochemical techniques. A mathematical model was developed to analyze the response of a conductometric enzyme biosensor for the detection of urea. The transducer is composed of interdigitated inert gold microelectrodes coated with a layer of urease enzyme. The main components of the biosensor are based on well-known physical processes such as diffusion as well as biological and electrochemical reactions. The finite difference method was used to solve partial differential equations coupling diffusive mass transfer to enzymatic kinetics. Experimental urea detection data were used to validate the mathematical model. The numerical results are compared with the experimental results and appear to be in good agreement. The responses of the biosensor to various conditions (such as the thickness of the diffusion layer, thickness of the enzyme

membrane, urea concentration, etc.) were simulated. This exploitation can guide experiments to improve analytical performance and reduce development costs.

2. Materials and Methods

2.1. Reagents and Apparatus

Bovine serum albumin (BSA), Urease (Type III from Jack Beans), glutaraldehyde (25% aqueous solution), glycerol (>99%) and phosphate buffered saline (PBS) were obtained from Sigma-Aldrich. All aqueous solutions were prepared using ultrapure water.

The conductometric transducers contain two identical pairs of gold interdigitated electrodes. The dimension of each interdigital space and digit was 20µm and the length of the digits was 1 mm. The area of each pair of electrodes was 1 mm². Measurements were performed at 23±2°C by applying to the differential pairs of electrodes an alternative voltage (10 mV amplitude, 100 kHz frequency) generated by a low-frequency wave form generator (SR830 lock-in amplifier from Stanford Research Systems).

2.2. Preparation of the urea biosensor

The suspension system contains 6% of BSA, 4% of urease and 10% of glycerol dispersing in 5 ml of phosphate buffer with a concentration of 20 mM (pH 7,3). The mixture was mixed for 1 hour. 0,2 µL of this solution was deposited onto interdigitated microelectrodes. For the preparation of the reference microelectrode, the same steps previously were followed, but in the absence of the urease in the initial mixture. The interdigitated microbiosensors were then placed in saturated glutaraldehyde vapours for 30 min. Finally, the biosensors were dried at room temperature for 30 min and stored at 4 °C before the experiments [17].

2.3. Conductometric measurements

Interdigitated microelectrodes modified by urease film were placed in a glass cell filled with 5 mL of PBS with a concentration of 5 mM (pH 7.3±0.1). The solution was stirred vigorously. Measurements were performed by applying to the differential pairs of electrodes an alternative voltage with the amplitude of 10mV and a frequency of 100 kHz generated by the generator. The measurements were repeated after adding urea to the PBS solution in a range of $1x10^{-8}$ to $3x10^{-6}$ mol/cm³. Experiments were carried out at ambient temperature.

3. Conductometric biosensor model

3.1. Description of the system

Urea in the bulk analyte solution diffuses through a diffusion boundary layer to the enzyme membrane, where its hydrolysis is catalyzed by urease. The ions formed by the reaction increase the electrical conductivity of the solution at the surface of the sensor. This change in conductivity is detected by a change in the electrical conductance of the array of interdigitated electrodes, which depends on the conductivity of the solution near the sensor surface. The concentrations of ionic products were used to calculate the spatial and temporal distribution of electrical conductivity.

The operation of the conductometric urea sensor was modeled by solving the coupled problem of mass transport and enzymatic reaction to determine the concentration of ionic products at the surface of the electrode.

The structure of the conductometric urea biosensor is illustrated schematically in Figure 1.For the development of a mathematical model it is assumed that, the geometry of the electrode is symmetrical. The enzyme membrane is uniform with a homogeneous distribution. It is also assumed that the transport process of all species is defined in a one-dimensional spatial domain.

The structure of the biosensor is divided into two zones; the diffusion layer from δ_m to δ_d where the bulk solution substrate diffuses without reaction, and the porous enzymatic membrane from 0 to δ_m where the substrate is hydrolyzed by urease immobilized to the electrode surface during diffusion.

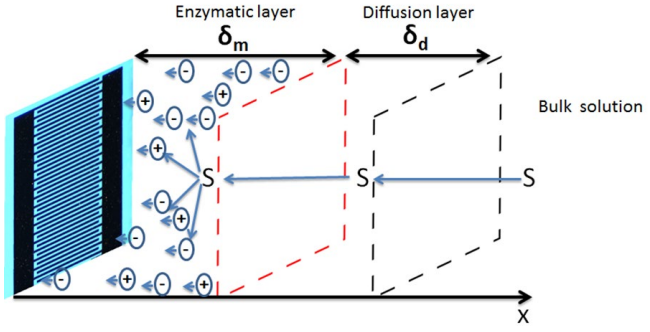

Figure 1. Scheme of principal structure of conductometric biosensor for urea detection. S: urea, positive and negative charges: product ions of the enzymatic reaction.

3.2. Enzymatic reaction

The detection principle due to ions generated by the hydrolysis of the urea catalysis by urease according to the reaction [4]:

$$CO(NH_2)_2 + 3H_2O \xrightarrow{Urease} 2NH_4^+ + HCO_3^- + OH^- \quad \text{Eq.1}$$

The enzymatic rate depends only on urea concentration; therefore the speed of the urease reaction can calculate according to the Michaelis-Menten mechanism [18]:

$$V = \frac{V_{max} \cdot S}{K_m + S} \quad \text{Eq.2}$$

Where V_{max} is the maximum of catalysis speed, K_m is Michaelis-Menten constant and S is the urea concentration at the sensor surface.

In the experiments conducted for this study, enzyme was immobilized only at the sensor surface, so the term V will be zero except at the sensor surface.

3.3. The kinetic paramaters of the enzymatic reaction

Figure 2 shows the graphic presentation of the linearization from the Michaelis-Menten equation:

$$\frac{1}{V} = \frac{K_m}{V_{max}}\frac{1}{S} + \frac{1}{V_{max}} \quad \text{Eq. 3}$$

The enzymatic speed corresponds to the slope of tangent at the origin [19]. The conductivity values at 120 s are considered to estimate the kinetic parameters of the urease enzyme immobilized to the sensor.

The linear equation found is $y = 7.72*10^{-7}\ x + 0.406$ with a correlation coefficient $R^2 = 0.998$. This linearization method gives the maximum of catalysis speed $V_{max} = 2.46$ µS $cm^{-1}.s^{-1}$ and the constant $K_m = 19.01*10^{-7}$ mol/cm^3.

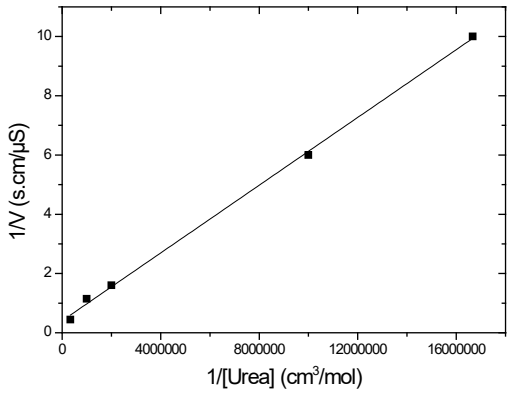

Figure 2. Lineweaver-Burk plot of urease kinetic for different urea concentrations.

3.4. Governing equations

For x ϵ] δ_m, δ_d [:

In the diffusion layer, concentrations of urea and products of enzymatic reaction depend on the time and position. The equations governing the system are based on the principle of conservation of mass. They can be described according to the second Fick's law by the following equations:

$$\frac{\partial S}{\partial t} = D_{sd}\frac{\partial^2 S}{\partial x^2} \quad \text{Eq.4}$$

$$\frac{\partial P}{\partial t} = D_{pd}\frac{\partial^2 P}{\partial x^2} \quad \text{Eq.5}$$

Where S: is the concentration of urea, P: is the concentration of the products of enzymatic reaction (NH_4^+; HCO_3^- ; OH^-), t: is the time, x: is the position and D_{sd}/D_{pd}: is Diffusivity of the substrate/products in the diffusion layer.

For x ϵ] 0, δ_m [:

In the enzymatic membrane, concentrations of urea and products of enzymatic reaction depend on the time, position and the rate of the enzymatic reaction. This system is described by the following mass balance equations:

$$\frac{\partial S}{\partial t} = D_{sm}\frac{\partial^2 S}{\partial x^2} - \frac{Vmax.\ S}{K_m+S} \quad \text{Eq.6}$$

$$\frac{\partial P}{\partial t} = D_{pm}\frac{\partial^2 P}{\partial x^2} + \upsilon_p\ \frac{Vmax.\ S}{K_m+S} \quad \text{Eq. 7}$$

Where υ_p: stoichiometric coefficients of the ion.

Initial conditions:

Initial conditions assume spatially uniform concentrations of all species; the initial conditions are as follows:

$$S(\delta_m+\delta_d,\ 0)=S_0 \quad \text{Eq.8}$$

$$S(x,0)=0 \quad \text{Eq. 9}$$

$$P(x,0)=0 \quad \text{Eq.10}$$

Where S_0 is the concentration of urea in bulk solution.

Boundary conditions:

At the diffusion layer-bulk solution interface ($x= \delta_m+ \delta_d$), the concentrations of the substrate and the products are equal to the bulk solution values during the biosensor operation:

$$S(\delta_m+\delta_d,t)=S_0 \quad \text{Eq.11}$$

$$P(\delta_m+\delta_d,t)=0 \quad \text{Eq.12}$$

At the enzymatic membrane-diffusion layer interface ($x= \delta_m$), the flux of substrate and products passing from one layer to another are assumed to be equal. This is defined by the following conditions (t> 0):

$$D_{sm}\frac{\partial S}{\partial x}\Big|_{x=\delta m} = D_{sd}\frac{\partial S}{\partial x}\Big|_{x=\delta m} \quad \text{Eq.13}$$

$$D_{pm}\frac{\partial P}{\partial}\Big|_{x=\delta m} = D_{pd}\frac{\partial P}{\partial x}\Big|_{x=\delta m} \quad \text{Eq.14}$$

At the electrode surface (x=0), the substrate is electro-inactive substance, and the concentration of the products at the sensor surface is being permanently reduced to zero due to the polarization of the electrode (t> 0) [18,20]:

$$\frac{\partial S}{\partial x}\Big|_{x=0} = 0 \quad \text{Eq.15}$$

$$P(0,t)=0 \quad \text{Eq.16}$$

The conductivity response of the biosensor was calculated using equation 17 below [21]:

$$\sigma_i^j = \sum_n |Z_n| \lambda_n P_{ni}^j \quad \text{Eq.17}$$

Where σ_i^j: is the conductivity of the i^{th} layer at the j^{th} time ($\mu S.cm^{-1}$), Z_n: is the charge of ion n, λ_n: is the equivalent ionic molar conductivity of the ion n ($\mu S.cm^2.mol^{-1}$), P_{ni}^j: is the concentration of the ion n in the i^{th} layer at the j^{th} time ($mol.cm^{-3}$).

3.5. Numerical method

Finite difference method was used to solve simultaneously equations (4)-(16), to predict the response of the conductometric biosensor as a function of time.

In order to simplify the modeling: The diffusion coefficients of the ionic species in each diffusion layer are equal. The time step (Δt) and the space step (Δx) are the same in the two diffusion layers.

The approximation of the equations of substrate (S) and products (P) in diffusion layer and enzymatic layer were given as follows, respectively:

For xϵ] δ_m, δ_d [

$$-D_{sd}\frac{\Delta t}{\Delta x^2}S_{i-1}^{j+1} + (1 + 2D_{sd}\frac{\Delta t}{\Delta x^2})S_i^{j+1} - D_{sd}\frac{\Delta t}{\Delta x^2}S_{i+1}^{j+1} = S_i^j \quad \text{Eq. 18}$$

$$-D_{pd}\frac{\Delta t}{\Delta x^2}P_{i-1}^{j+1} + (1 + 2D_{pd}\frac{\Delta t}{\Delta x^2})P_i^{j+1} - D_{pd}\frac{\Delta t}{\Delta x^2}P_{i+1}^{j+1} = P_i^j \quad \text{Eq. 19}$$

For xϵ] 0, δ_m [

$$-\boldsymbol{D_{sm}\frac{\Delta t}{\Delta x^2}S_{i-1}^{j+1}} + (\mathbf{1} + \mathbf{2}\boldsymbol{D_{sm}\frac{\Delta t}{\Delta x^2}})\boldsymbol{S_i^{j+1}} - \boldsymbol{D_{sm}\frac{\Delta t}{\Delta x^2}S_{i+1}^{j+1}} = \boldsymbol{S_i^j} - \frac{\boldsymbol{V_{max}S_i^j}}{\boldsymbol{K_m + S_i^j}} \quad \text{Eq. 20}$$

$$-\boldsymbol{D_{pm}\frac{\Delta t}{\Delta x^2}P_{i-1}^{j+1}} + \left(\mathbf{1} + \mathbf{2}\boldsymbol{D_{pm}\frac{\Delta t}{\Delta x^2}}\right)\boldsymbol{P_i^{j+1}} - \boldsymbol{D_{pm}\frac{\Delta t}{\Delta x^2}P_{i+1}^{j+1}} = \boldsymbol{P_i^j} + \boldsymbol{v_p}\frac{\boldsymbol{V_{max}S_i^j}}{\boldsymbol{K_m + S_i^j}} \quad \text{Eq. 21}$$

The initial and boundary conditions are approximated as follows:

For t = 0

$$\boldsymbol{S_{end}^0 = S_0} \quad \text{Eq. 22}$$

$$\boldsymbol{S_i^0 = 0} \quad \text{Eq. 23}$$

$$\boldsymbol{P_i^0 = 0} \quad \text{Eq. 24}$$

For x = 0

$$\boldsymbol{S_0^j = S_1^j} \quad \text{Eq. 25}$$

$$\boldsymbol{P_0^j = 0} \quad \text{Eq.26}$$

For x = δ_m

$$\boldsymbol{S_i^j = \frac{D_{sm}S_{i-1}^j + D_{sd}S_{i+1}^j}{D_{sm} + D_{sd}}} \quad \text{Eq. 27}$$

$$\boldsymbol{P_i^j = \frac{D_{pm}P_{i-1}^j + D_{pd}P_{i+1}^j}{D_{pm} + D_{pd}}} \quad \text{Eq. 28}$$

For x = δ_m+δ_d

$$\boldsymbol{P_{end}^j = S_0} \quad \text{Eq. 29}$$

$$\boldsymbol{P_{end}^j = 0} \quad \text{Eq. 30}$$

Where: i ranging from 0 to $(\delta_m+\delta_d)/\Delta x$, and j ranging from 0 to final time/Δt.

3.6. Numerical simulation

At each time step, discretized version of different equations was solved applying Thomas algorithm [22]. The numerical simulation of the biosensor responses has been carried out using Matlab software. The unknown parameters (δ_m, δ_d, D_{sd}, D_{sm}, D_{pd}, D_{pm}) are determined by minimizing the error between the experimental and the theoretical values of the conductivity. This error is calculated according to the following relationship.

$$e = \sum \left| \frac{\sigma_{theoretical} - \sigma_{experimental}}{\sigma_{theoretical}} \right| \quad \text{Eq. 31}$$

The general algorithm of the simulation is represented in Figure 3, and the parameters used during this simulation are gathered in Table 1.

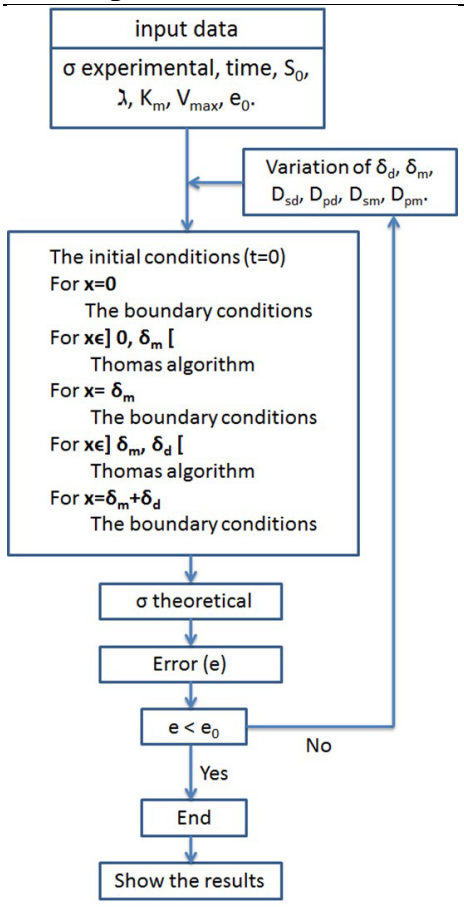

Figure 3. Simulation algorithm of the mathematical model.

4. Results and Discussion

4.1. Model Validation

The various parameters of the conductometric biosensor determined by the model for the different concentrations of urea are gathered in Table 2. The diffusion layer and the thickness of the enzymatic membrane are estimated at 0.0022 cm and 0.0211 cm, respectively. The values of diffusion coefficient of the substrate in the diffusion layer (D_{sd}) was between 1.40 10^{-8} and 2.23 10^{-8}cm²/s (D_{sd} medium = 2.23 10^{-8}cm²/s). The diffusivity of urea in the enzymatic layer was estimated between 9.50 10^{-7} and 4.12 10^{-7} cm²/s (D_{sm} medium = 6.81 10^{-7}cm²/s). For the products, the diffusion coefficient in the enzymatic membrane is approximated to a value between 4.20 10^{-8} and 7.10 10^{-8} cm²/s (D_{pm} medium = 5.65 10^{-8}cm²/s). While, the diffusivity value of the products in the diffusion layer is negligible (D_{pd} <10^{-22}cm²/s).

The numerical simulation of the mathematical model previously described was successfully applied to calibrate the response of the urea biosensor. Figure 4.a shows that a better fit is achieved between the experimental and theoretical data with an adjustment error less than 10^{-3}. Considering the steady state conductivity, a good linear relationship between the experimental and theoretical conductivity as a function of the urea concentration is achieved (Fig.4.b). The regression equations are σ = 0.107*10^8 [urea] + 19,4; R^2=0.96 and σ = 0.106*10^8 [urea] + 21.4; R^2=0.97; respectively with a 1.80% relative standard deviation.

Table 1. Parameters and variables used in the numerical simulation.

Parameters/Variables	Dimensional parameters	Value/Variation range
Time	t, s	0-630
Diffusion layer thickness	δ_d, cm	0.0001-0,01
Enzymatic layer thickness	δ_m, cm	0.0001-0,01
Initial concentration of urea	S_0, mol/cm³	1*10^{-8}-3*10^{-6}
Michaelis-Menten constant	K_m, mol/cm³	19.01*10^{-7}
Maximum of catalysis speed	V_{max}, µS/cm.s	2,46
Diffusivity of the substrate in the diffusion layer.	D_{sd}, cm²/s	10^{-6}-10^{-9}
Diffusivity of the products in the diffusion layer.	D_{pd}, cm²/s	10^{-6}-10^{-9}
Diffusivity of the substrate in the enzymatic layer.	D_{sm}, cm²/s	10^{-6}-10^{-9}
Diffusivity of the products in the enzymatic layer.	D_{pm}, cm²/s	10^{-6}-10^{-9}
Equivalent ionic molar conductivity of NH_4^+/HCO_3^-/OH^-	ƛ, µS.cm²/mol	7350/4450/19800
Experimental conductivity	σ, µS/cm	/

Table 2. Different parameters of the conductometric biosensor estimated by the model for different concentrations of urea.

Concentration (mol/cm³)	D_{sd} (cm²/s)	D_{sm} (cm²/s)	D_{pm} (cm²/s)	δ_d (cm)	δ_m (cm)	error
$1x10^{-8}$	$2.23\ 10^{-8}$	$9.50\ 10^{-7}$	$4.20\ 10^{-8}$	0.0022	0.0211	$3.12\ 10^{-4}$
$6x10^{-8}$	$1.65\ 10^{-8}$	$6.05\ 10^{-7}$	$4.50\ 10^{-8}$	0.0022	0.0211	$1.75\ 10^{-4}$
$1x10^{-7}$	$1.50\ 10^{-8}$	$5.75\ 10^{-7}$	$4.80\ 10^{-8}$	0.0022	0.0211	$3.66\ 10^{-4}$
$2,5x10^{-7}$	$1.90\ 10^{-8}$	$5.05\ 10^{-7}$	$5.30\ 10^{-8}$	0.0022	0.0211	$1.78\ 10^{-4}$
$5x10^{-7}$	$1.40\ 10^{-8}$	$5.25\ 10^{-7}$	$6.10\ 10^{-8}$	0.0022	0.0211	$5.76\ 10^{-4}$
$1x10^{-6}$	$1.60\ 10^{-8}$	$4.65\ 10^{-7}$	$6.50\ 10^{-8}$	0.0022	0.0211	$4.32\ 10^{-4}$
$3x10^{-6}$	$1.80\ 10^{-8}$	$4.12\ 10^{-7}$	$7.10\ 10^{-8}$	0.0022	0.0211	$1.42\ 10^{-4}$

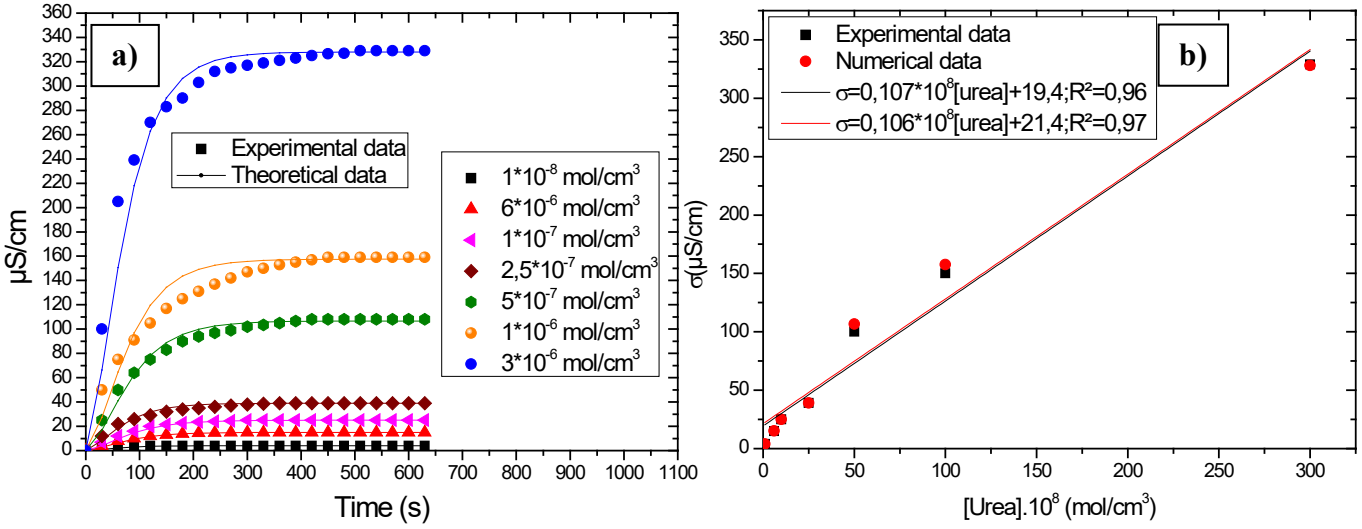

Figure 4. a) Theoretical results and the experimental data of the conductometric biosensor response for different concentrations of urea. **b)** Experimental and numerical calibration curves of the conductometric urea biosensor

4.2. Model exploitation

4.2.2. Concentration and conductivity profiles

By using the mathematical model developed, it is possible to determine the concentrations of the substrate and the products as a function of time in the vicinity of the electrodes.

Figure 5 shows the variation of the concentration of urea in the diffusion layer and the enzymatic membrane for a concentration of urea in solution equal to $S_0 = 3*10^{-6}$. The concentration of urea at $x = \delta_m + \delta_d$ equal to S_0. At $x = \delta_m + 9/10\ \delta_d$, the concentration of urea in steady state ($2.279*10^{-7}$ mol/cm³) is 13.16 times weaker than S_0. Urea concentration continues to decrease, at $x = \delta_m$ the steady-state concentration equal to $4.294*10^{-8}$ mol/cm³, this value is 69.86 times weaker than S_0.

In the enzyme membrane, at $x = 9/10\ \delta_m$ the concentration of urea in steady state equal to $2.377*10^{-8}$ mol/cm³, it is 128.21 times weaker than S_0 and 1.8 times weaker than the value at $x = \delta_m$. The urea concentration is lower and lower for an x close to zero, at x=0 it is equal to $1.897*10^{-10}$ mol/cm³, that is to say it is 15814.4 more weaker than S_0.

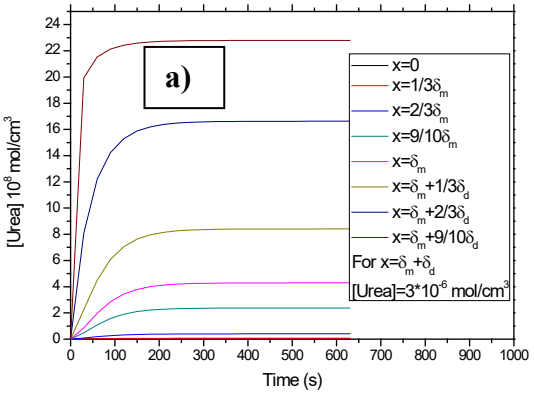

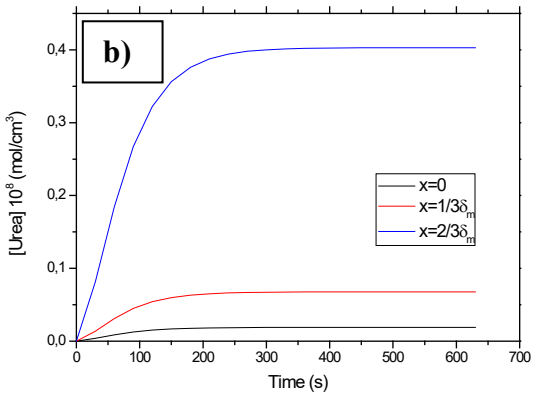

Figure 5. a) Urea concentration profiles in the diffusion layer and in the enzyme membrane for S_0=3x10^{-6} mol/cm^3. **b)** Enlargement of figure 5.a.

In another side, the figure 6.a represents the concentration profiles of HCO_3^- and OH^-, and the figure 6.b represents the concentration profiles of the NH_4^+ in the enzyme membrane. This difference is due to the stoichiometric coefficients. The concentrations of the products of the enzymatic reaction in steady state are maximum for x = δ_m, such that [HCO_3^-] = [OH^-] = 0.5824 mol/cm^3 and [NH_4^+] = 1.1647 mol/cm^3. These concentrations decrease as they approach the surface of the electrode. They are 3.3 more weaker at x = 2/3 δ_m, 18.4 more weaker at x = 1/3 δ_m and 69.3 more weaker at the electrode surface.

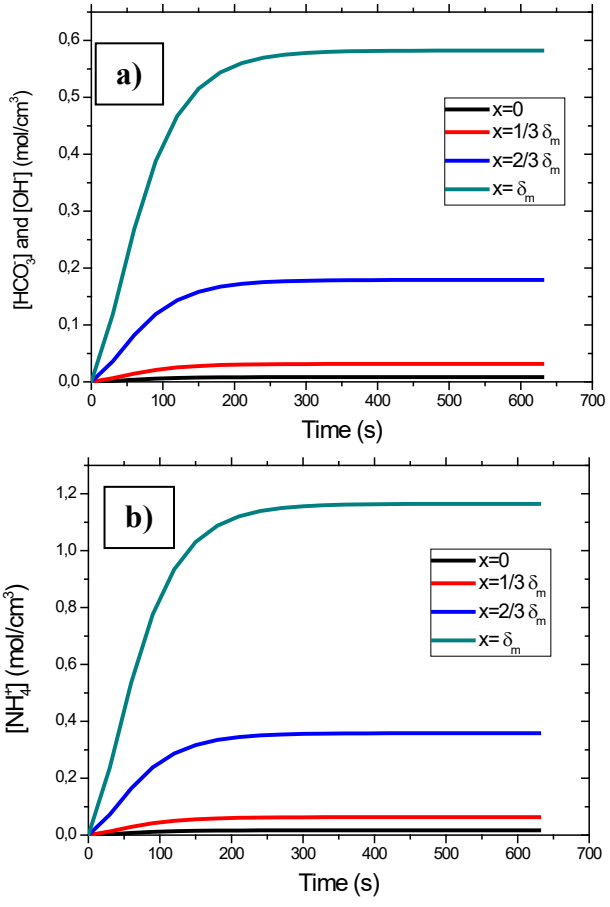

Figure 6. a) HCO_3^- and OH^- concentration profiles **b)** NH_4^+ concentration profiles: in the enzyme membrane for S_0=3*10^{-6} mol/cm^3.

The concentration profiles made it possible to see how conductivity varies as a function of time and distance x. Figure 7 represents the conductivity at different points in the enzyme membrane. The conductivity in steady state is maximum at x = δ_m (σ = 27241 µS/cm). Conductivity values decrease as they approach the surface of the electrode. In steady state, it takes a value of 6967.4 µS/cm at x = 2/3 δ_m, 1226.3 µS/cm at x = 2/3 δ_m and 327,975 µS/cm at the surface of the electrode.

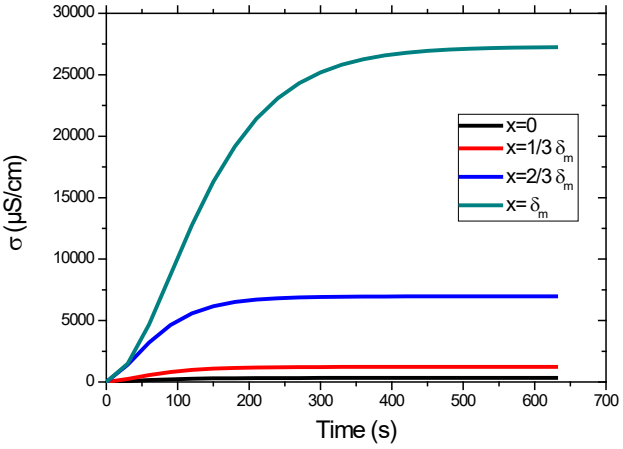

Figure 7. Conductivity profiles in the enzyme membrane for S_0=3*10^{-6} mol/cm^3.

4.2.2. Influence of diffusion layer and enzyme membrane thicknesses

The study of the conductivity in function of time was performed using different values of diffusion layer thickness (δ_d) (from 2 to 40 µm) for S_0= 3*10^{-6} mol/cm^3, δ_m=0.02cm, D_{sd}=2*10^{-8} cm²/s, D_{sm}=4*10^{-7} cm²/s, D_{pd}=10^{-22} cm²/s and D_{pm}=7*10^{-8} cm²/s (Fig.8.a). For small values of diffusion layer thickness, the conductivity of the biosensor is bigger and increases rapidly until to reach the steady state condition. For greater value of diffusion layer thickness, the conductivity of the biosensor decrease, and the time required to establish the steady state increases. This behavior because the concentration gradient that is established in the diffusion layer is greater for greater thicknesses. Based on these observations, it is recommended to keep the detection enclosure stirred. It is preferable to use maximum agitation possible in order to further reduce the thickness of the diffusion layer. This agitation should not be greater in order to avoid affecting the enzyme membrane.

In addition to the diffusion layer effect, the thickness of the enzyme membrane can also affect the response of the biosensor. Figure 8.b represents the study of the

conductivity in function of time using different values of enzyme membrane thickness (δ_m) (from 100 to 300 µm) for δ_d=0,002cm, $D_{sd}=2*10^{-8}$ cm²/s, $D_{sm}=4*10^{-7}$ cm²/s, $D_{pd}=10^{-22}$ cm²/s and $D_{pm}=7*10^{-8}$ cm²/s. The conductivity is inversely proportional to the thickness of the enzyme membrane. It is larger with a thinner enzymatic membrane and it is weak with a thicker enzyme membrane. For the thick films, the effect of the resistance to mass transfer in the membrane enzyme becomes important, and then the resistance to mass transfer in the enzyme membrane decreases with the decrease in the thickness of the membrane.

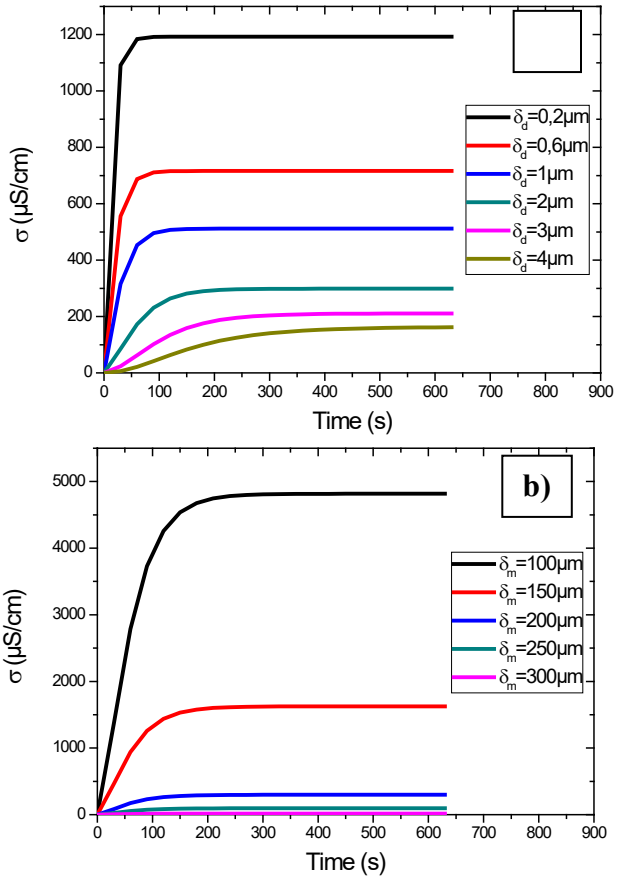

Figure 8. a) The effect of diffusion layer on the conductometric response of the biosensor for S_0= $3*10^{-6}$ mol/cm³, V_{max}=2.46 µS/cm.s, $K_m=19.01*10^{-7}$ mol/cm³, δ_m=0.02cm, $D_{sd}=2*10^{-8}$ cm²/s, $D_{sm}=4*10^{-7}$ cm²/s, $D_{pd}=10^{-22}$ cm²/s and $D_{pm}=7*10^{-8}$ cm²/s. **b)** The effect of enzyme membrane on the conductometric response of the biosensor for S_0= $3*10^{-6}$ mol/cm³, V_{max}=2.46 µS/cm.s, $K_m=19.01*10^{-7}$ mol/cm³, δ_d=0.002cm, $D_{sd}=2*10^{-8}$ cm²/s, $D_{sm}=4*10^{-7}$ cm²/s, $D_{pd}=10^{-22}$ cm²/s and $D_{pm}=7*10^{-8}$ cm²/s.

4.2.3. Influence of urea concentration (S_0)

In figure 9 is shown the conductometric response of the biosensor for different values of the concentration of urea in solution from 10^{-9} to 3 mol/cm³ for δ_d=0.002cm, δ_m=0.02cm, $D_{sd}=2*10^{-8}$ cm²/s, $D_{sm}=4*10^{-7}$ cm²/s, $D_{pd}=10^{-22}$ cm²/s and $D_{pm}=7*10^{-8}$ cm²/s. It is observable that for the lowest concentrations (<10^{-8} mol/cm³) the conductivity is almost zero. With increasing concentration from 10^{-8} to 1 mol/cm³, conductivity significantly increases and the time required to establish the steady state decreases. Then, for higher concentrations (>1 mol/cm³) the conductivity is maximum and almost without variation.

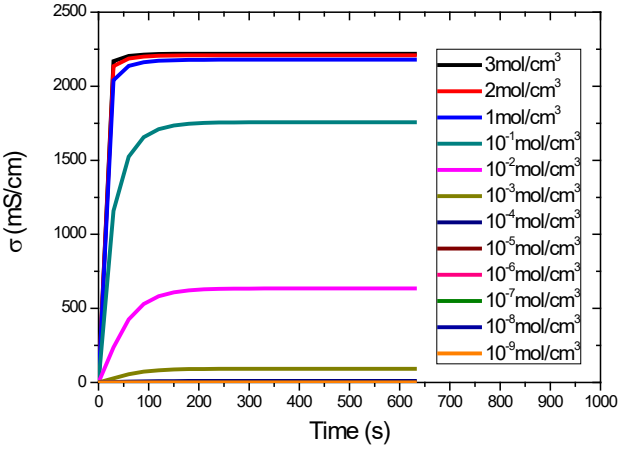

Figure 9. The effect urea concentration on the conductometric response of the biosensor for V_{max}=2.46 µS/cm.s, $K_m=19.01*10^{-7}$ mol/cm³, δ_d=0.002cm, δ_m=0.02cm, $D_{sd}=2*10^{-8}$ cm²/s, $D_{sm}=4*10^{-7}$ cm²/s, $D_{pd}=10^{-22}$ cm²/s and $D_{pm}=7*10^{-8}$ cm²/s.

For the highest concentrations of urea in solution, figure 10.a shows the concentration profiles of urea and figure 10.b shows the concentration profiles of OH^- in the enzyme membrane determined by the mathematical model using two high concentrations of urea in solution 2 and 3 mol/cm³ for δ_d=0.002cm, δ_m=0,02cm, $D_{sd}=2*10^{-8}$ cm²/s, $D_{sm}=4*10^{-7}$ cm²/s, $D_{pd}=10^{-22}$ cm²/s and $D_{pm}=7*10^{-8}$ cm²/s. At each position of x, the urea concentration is large if S_0 is large (fig.10.a). This indicates that the substrate is present in the enzyme membrane and its concentration is proportional to S_0.

But the concentrations of OH^- are the same for each position in the enzymatic membrane whatever the S_0 concentration in solution (fig 10.b). This indicates that the enzyme is saturated and its activity is maximum. It is for this reason that the conductivity of passes varies with the large concentrations S_0. In this case to significantly detect large concentrations it is recommended to use a higher enzyme concentration.

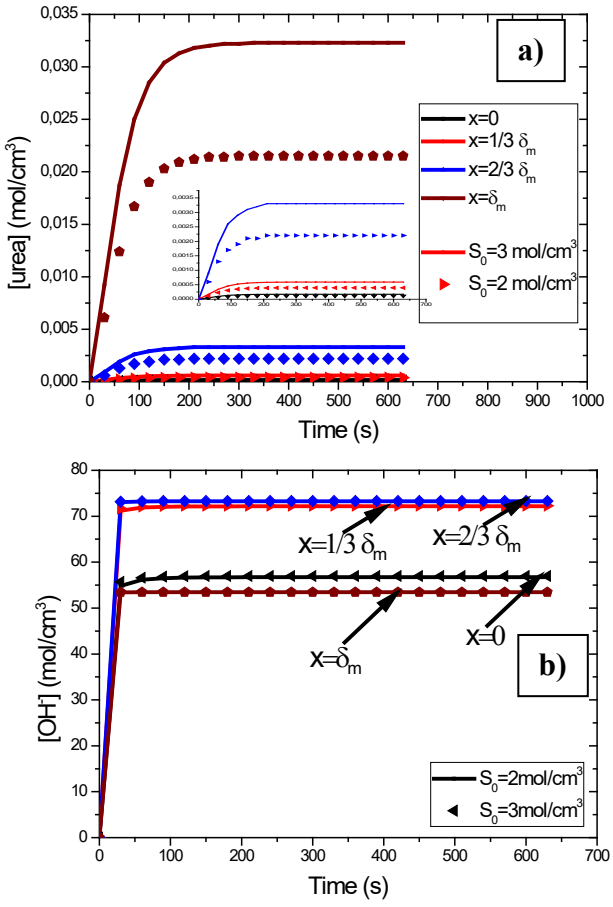

Figure 10. a) Urea concentration profiles **b)** OH^- concentration profiles: in the enzyme membrane with S_0=2 mol/cm³ and S_0=3 mol/cm³ for V_{max}=2.46 µS/cm.s, K_m=19.01*10^{-7} mol/cm³, δ_d=0.002cm, δ_m=0.02cm, D_{sd}=2*10^{-8} cm²/s, D_{sm}=4*10^{-7} cm²/s, D_{pd}=10^{-22} cm²/s and D_{pm}=7*10^{-8} cm²/s.

The substrate and product concentration profiles were studied in order to understand why the conductivity is almost zero with low concentrations and why it does not vary with high concentrations.

Figure 11.a shows the concentration profiles of urea and figure 11.b shows the concentration profiles of OH^- in the enzyme membrane determined by the mathematical model using two low concentrations of urea in solution 10^{-8} and 10^{-9} mol/cm³ for δ_d=0,002cm, δ_m=0.02cm, D_{sd}=2*10^{-8} cm²/s, D_{sm}=4*10^{-7} cm²/s, D_{pd}=10^{-22} cm²/s and D_{pm}=7*10^{-8} cm²/s.

With low concentrations S_0 in solution, the concentration of urea (fig.11.a) and products (fig.11.b) at x=0 is almost negligible which explains the absence of the conductometric response. But at the same position of x close to δ_m, the urea and product concentrations for S_0= 10^{-8} mol/cm³ are greater than that for S_0= 10^{-9} mol/cm³. Therefore to have a significant signal and to move towards the detection of very low concentrations, it is recommended to use a thin enzymatic membrane.

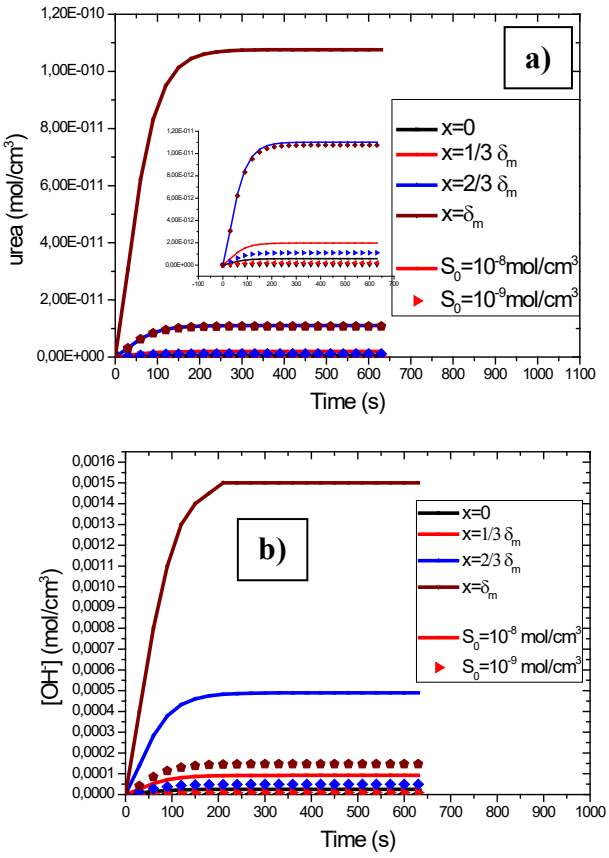

Figure 11. a) Urea concentration profiles **b)** OH^- concentration profiles: in the enzyme membrane with S_0=10^{-8} mol/cm³ and S_0=10^{-9} mol/cm³ for V_{max}=2.46 µS/cm.s, K_m=19.01*10^{-7} mol/cm³, δ_d=0.002cm, δ_m=0.02cm, D_{sd}=2*10^{-8} cm²/s, D_{sm}=4*10^{-7} cm²/s, D_{pd}=10^{-22} cm²/s and D_{pm}=7*10^{-8} cm²/s.

4.2.4. Effects of the maximum enzymatic rate V_{max}

Figure 12 shows the variation in conductivity as a function of the maximum enzymatic rate. This study shows that the conductivity is proportional to V_{max}. Such that more than V_{max} is large, the sensitivity of the sensor is stronger. Practically, it is possible to accelerate the rate of the reaction by increasing the concentration of the enzyme in the membrane or else by increasing the temperature on condition that it does not go beyond the denaturation temperature [23].

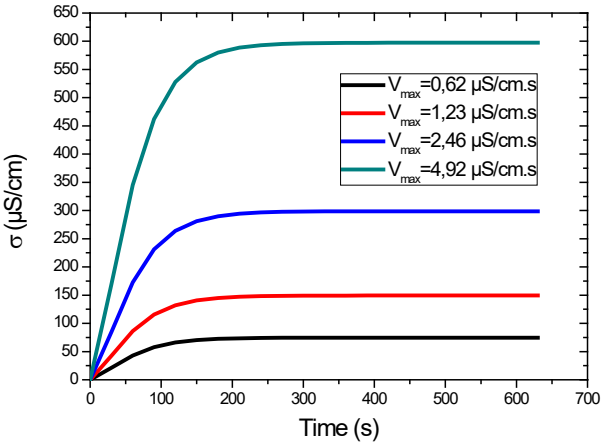

Figure 12. The effect of the maximum enzymatic rate (V_{max}) on the conductometric response of the biosensor for K_m=19.01*10^{-7} mol/cm^3, δ_d=0.002 cm, δ_m=0.02 cm, D_{sd}=2*10^{-8} cm²/s, D_{sm}=4*10^{-7} cm²/s, D_{pd}=10^{-22} cm²/s and D_{pm}=7*10^{-8} cm²/s.

4.2.5. Effects of the kinetic constant K_m

The response of the sensor also depends on the value of the kinetic constant. Figure 13 summarizes the conductometric responses for different values of the kinetic constant, where conductivity is plotted against time. For higher values of Km, the conductivity increases only slightly. This generally reflects a low sensitivity to urea. For lower values of K the signal rises higher. This shows that the sensitivity of the sensor for urea is very high. The kinetic constant is a parameter which can, in practice, be difficult to modify substantially [20]

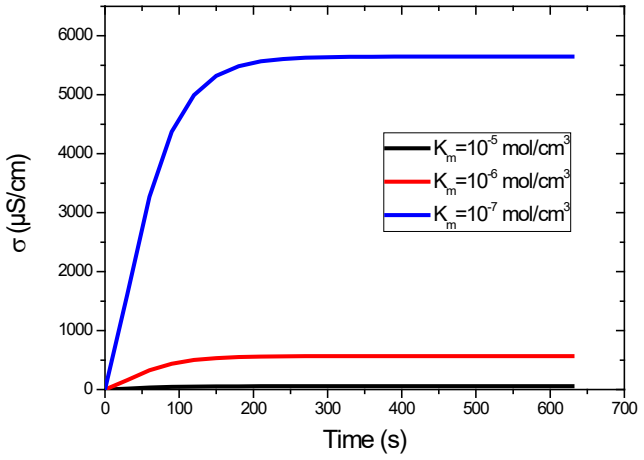

Figure 13. The effect of the kinetic constant (K_m) on the conductometric response of the biosensor for V_{max}=2.46 µS/cm.s, δ_d=0.002cm, δ_m=0.02cm, D_{sd}=2*10^{-8} cm²/s, D_{sm}=4*10^{-7} cm²/s, D_{pd}=10^{-22} cm²/s and D_{pm}=7*10^{-8} cm²/s.

5. Conclusion

In this paper, a mathematical model was developed to simulate the response of the conductometric biosensor for the detection of urea. It is based on an interdisciplinary approach which combines the law of diffusion, the enzymatic kinetics of Michaelis-Menten, numerical methods, electrochemistry and computer science. The model has been successfully applied to describe the enzymatic reaction/diffusion system of the urea biosensor. The presented study demonstrates that the model developed could also be used to predict the conductometric response as a function of the various parameters which allows to guide the experiments, and to optimize the biosensor by improving these analytical characteristics and reducing development costs.

6. Acknowledgements

The authors acknowledge the financial support of the EU H2020 WIDESPREAD Program entitled Bionanosens grant agreement # 951887.

7. References

[1] A. Soni, R.K. Surana, S.K.Jha, *Sensors and Actuators B: Chemical* **2018**, *269*, 346–353.
[2] M. Khan, Y. Kim, J.H. Lee, I.K. Kang, S.Y. Park, *Anal. Methods* **2014**, *6*, 5753–5759.
[3] A.A. Ibrahim, R. Ahmad, A. Umar, M.S. Al-Assiri, A.E. Al-Salami, R. Kumar, S.G. Ansari, S. Baskoutas, *Biosensors and Bioelectronics* **2017**, *98*, 254–260.
[4] M. Singh, N. Verma, A. Garg, N. Redhu, *Sensors and Actuators B: Chemical* **2008**, *134*, 345–351.
[5] Z. Gharsallah, M. Najjar, B. Suthar, V. Janyani, *Optical and Quantum Electronics* **2018**, *50*, 1–10.
[6] S. Botewad, V. Pahurkar, G. Muley, *Optical Fiber Technology* **2018**, *40*, 8–12.
[7] C.Y.K. Lai, P.J. Foot, J.W. Brown, P. Spearman, *Biosensors* **2017**, *7*, 13.
[8] K. Sihombing, M.C. Tamba, W.S. Marbun, M. Situmorang, Indian Journal of Chemistry **2018**, *57A*, 175-180.
[9] F. Jannah, J.M. Kim, *Dyes and Pigments* **2019**, *169*, 15–21.
[10] M.C. Tavares, K.A. Oliveira, A. de Fátima, W.K. Coltro, J.C.C. Santos, *Talanta* **2021**, 122301.
[11] B. Sahin, T. Kaya, *Materials Research Express* **2019**, *6*, 042003.
[12] M. Dervisevic, E. Dervisevic, M. Şenel, *Sensors and Actuators B: Chemical* **2018**, *254*, 93–101.
[13] S.K. Kirdeciler, E. Soy, S. Öztürk, I. Kucherenko, O. Soldatkin, S. Dzyadevych, B. Akata, *Talanta* **2011**, *85*, 1435–1441.
[14] T. Velychko, O. Soldatkin, V. Melnyk, S. Marchenko, S. Kirdeciler, B. Akata, A. Soldatkin, A. El'skaya, S. Dzyadevych, *Nanoscale research Letters* **2016**, *11*, 1–6.

[15] S. Dzyadevych, N. Jaffrezic-Renault, Conductometric biosensors. In *Biological Identification*; Elsevier, 2014; pp. 153–193.
[16] N. Jaffrezic-Renault, S.V. Dzyadevych, *Sensors* **2008**, *8*, 2569–2588.

[17] W. Nouira, A. Maaref, F. Vocanson, M. Siadat, J. Saulnier, F. Lagarde, N. Jaffrezic-Renault, *Electroanalysis* **2012**, *24*, 1088–1094.
[18] F. Achi, S. Bourouina-Bacha, M. Bourouina, A. Amine, *Sensors and Actuators B: Chemical* **2015**, *207*, 413–423.
[19] Y. Braham, H. Barhoumi, A. Maaref, *Analytical Methods* **2013**, *5*, 4898–4904.
[20] J.K. Leypoldt, D.A. Gough, D.A. *Analytical Chemistry* **1984**, *56*, 2896–2904.
[21] N.F. Sheppard Jr, D.J. Mears, A. Guiseppi-Elie, *Biosensors and Bioelectronics* **1996**, *11*, 967–979.
[22] W. Lee, Tridiagonal Matrices: Thomas Algorithm. *MS6021, Scientific Computation, University of Limerick* **2011**.
[23] G. Shu, B. Zhang, Q. Zhang, H. Wan, H. Li, *Acta Universitatis Cibiniensis. Series E: Food Technology* **2016**, *20*, 29–38.